blood advances

American Society of Hematology
2021 L Street NW, Suite 900,
Washington, DC 20036
Phone: 202-776-0544 | Fax 202-776-0545
bloodadvances@hematology.org

Development of combination therapies with BTK inhibitors and dasatinib to treat CNS-infiltrating E2A-PBX1+/preBCR+ ALL

Tracking no: ADV-2023-011582R2

Gaia Gentile (University of Freiburg Medical Center, Germany) Teresa Poggio (University Medical Center Freiburg, Germany) Antonella Catalano (University Medical Center Freiburg, Germany) Minna Voutilainen (Institute of Biomedicine, School of Medicine, University of Eastern Finland, Kuopio, Finland, Finland) Mari Lahnalampi (Institute of Biomedicine, School of Medicine, University of Eastern Finland, Kuopio, Finland, Finland) Marta Andrade-Martinez (University of Freiburg Medical Center, Germany) Tobias Ma (University of Freiburg Medical Center, Germany) Roman Sankowski (Faculty of Medicine, University of Freiburg, Germany) Lina Goncharenko (University of Freiburg Medical Center, Germany) Stefan Tholen (University of Freiburg Medical Center, Germany) Kyuho Han (MEDIC LIFE SCIENCES, United States) David Morgens (Stanford University, United States) Marco Prinz (University of Freiburg, Germany) Michael Lübbert (University of Freiburg, Germany) Sophia Engel (University of Freiburg Medical Center, Germany) Tanja Hartmann (Faculty of Medicine and Medical Center, University of Freiburg, Freiburg, Germany, Germany) Gunnar Cario (Children's Hospital, University Medical Center Schleswig-Holstein, Kiel, Germany, Germany) Martin Schrappe (University Medical Center Schleswig-Holstein, Campus Kiel, Germany) Lennart Lenk (Christian-Albrechts University Kiel and University Medical Center Schleswig-Holstein, Kiel, Germany, Germany) Martin Stanulla (Hannover Medical School, Germany) Justus Duyster (University Medical Center Freiburg, Germany) Peter Bronsert (University of Freiburg Medical Center, Germany) Michael Bassik (Stanford University Medical Center,) Michael Cleary (Stanford University School of Medicine, United States) oliver schilling (University Medical Center Freiburg, Germany) Merja Heinäniemi (University of Eastern Finland, Finland) Jesus Duque-Afonso (University of Freiburg Medical Center, Germany)

Abstract:
The t(1;19) translocation, which codes for the oncogenic fusion protein E2A (TCF3)-PBX1, is involved in acute lymphoblastic leukemia (ALL) and associated with a pre-B cell receptor (preBCR+) phenotype. Relapse in E2A-PBX1+ ALL patients frequently occurs in the central nervous system (CNS). Therefore, there is a medical need for the identification of CNS active regimens for the treatment of E2A-PBX1+/preBCR+ ALL. Using unbiased shRNA library screening approaches, we identified Bruton's tyrosine kinase (BTK) as a key gene involved in both proliferation and dasatinib sensitivity of E2A-PBX1+/preBCR+ ALL. Depletion of BTK by shRNAs resulted in decreased proliferation of dasatinib-treated E2A-PBX1+/preBCR+ cells compared with control-transduced cells. Moreover, combination of dasatinib with BTK inhibitors (BTKi) (ibrutinib, acalabrutinib or zanubrutinib) significantly decreased E2A-PBX1+/preBCR+ human and murine cell proliferation, reduced PLCG2 and BTK phosphorylation and total protein levels and increased disease-free survival of mice in secondary transplantation assays, reducing particularly CNS-leukemic infiltration. Hence, dasatinib with ibrutinib reduced pPLCG2 and pBTK in primary ALL patient samples, including E2A-PBX1+ ALLs. In summary, genetic depletion and pharmacological inhibition of BTK increase dasatinib effects in human and mouse E2A-PBX1+/preBCR+ ALL in most of performed assays, and the combination of dasatinib and BTKi is very effective in reducing CNS-infiltration of E2A-PBX1+/preBCR+ ALL cells in vivo.

Conflict of interest: COI declared - see note

COI notes: The authors declare no potential conflict of interest with the submission of the abstract. J.D.-A. received speakers honoraria from Riemser, Lilly, Ipsen, Roche, Amgen and AstraZeneca and travel support from Astra Zeneca, Ipsen, Gilead and Sobi.ML received research support from Janssen-Cilag.

Preprint server: No;

Author contributions and disclosures: GG planned and performed the experiments. JD-A designed the experiments. GG and TP performed mouse experiments. GG and AC performed immunohistochemical stainings. MP, DWM and RS prepared the paraffin-embedded mice samples blocks. MLü and TM provided reagents. GG and TM prepared the RNA samples for sequencing. MH, MLa and MV analyzed the RNA sequencing data. GG and MAM performed the phospho-specific flow cytometry (phospho-flow). GG and TP performed the phospho-flow on primary samples. MCB, KH and DWM designed, performed and analyzed the data from shRNA library screen assay. LL, GC, MS, MS and JDu provided patient samples. MLC provided mouse E2A-PBX1+ leukemia cells. GG and JD-A wrote the manuscript and prepared the figures. All authors revised the final version of the paper. All authors have read and agreed to the published version of the manuscript

Non-author contributions and disclosures: No;

Agreement to Share Publication-Related Data and Data Sharing Statement: The data generated during and/or analyzed during the current study are available upon reasonable request from the corresponding author. The bulk RNA sequencing data has been deposited in Gene Expression Omnibus under the following accession number GSE221238, token clkhwucmttejpaf (http://ncbi.nlm.nih.gov/geo).

Clinical trial registration information (if any):

Development of combination therapies with BTK inhibitors and dasatinib to treat CNS-infiltrating E2A-PBX1+/preBCR+ ALL

Short title

Targeted therapies for E2A-PBX1^{+}/preBCR^{+} ALLs

Authors

Gaia Gentile[1], Teresa Poggio[1], Antonella Catalano[1], Minna Voutilainen[2], Mari Lahnalampi[2], Marta Andrade-Martinez[1], Tobias Ma[1], Roman Sankowski[3], Lina Goncharenko[4,5,12], Stefan Tholen[5,12], Kyuho Han[6], David W. Morgens [6], Marco Prinz[3,10,11], Michael Lübbert[1], Sophia Engel[1], Tanja Nicole Hartmann[1], Gunnar Cario[8], Martin Schrappe[8], Lennart Lenk[8], Martin Stanulla[9], Justus Duyster[1], Peter Bronsert[5], Michael C. Bassik[6], Michael L. Cleary[7], Oliver Schilling[4,5,12], Merja Heinäniemi[2], Jesús Duque-Afonso[1]

Affiliations

[1] Department of Hematology and Oncology, University Medical Center Freiburg, Faculty of Medicine, University of Freiburg, Freiburg, Germany

[2] Institute of Biomedicine, School of Medicine, University of Eastern Finland, Kuopio, Finland

[3] Department of Neuropathology, University of Freiburg Medical Center, Faculty of Medicine, University of Freiburg, Freiburg, Germany

[4] Institute for Molecular Medicine and Cell Research, Faculty of Medicine, University of Freiburg, Freiburg, Germany.

[5] Institute of Surgical Pathology, University of Freiburg Medical Center, Faculty of Medicine, University of Freiburg, Freiburg, Germany.

[6] Department of Genetics, Stanford University School of Medicine, Stanford, CA, USA

[7] Department of Pathology, Stanford University School of Medicine, Stanford, CA, USA

[8] Department of Pediatrics, University Medical Center Schleswig-Holstein, Campus Kiel, Kiel, Germany

[9] Department of Pediatrics, University Medical Center Hannover, Hannover, Germany

[10] Center for NeuroModulation, Faculty of Medicine, University of Freiburg, Freiburg, Germany

[11] Signaling Research Centers BIOSS and CIBSS, University of Freiburg, Freiburg, Germany

[12] Proteomic Core Facility (ProtCF), Medical Center – University of Freiburg, Faculty of Medicine, University of Freiburg, Germany.

Key Points

Genetic and pharmacological inhibition of BTK increases dasatinib sensitivity *in vitro and in vivo* including in E2A-PBX1^{+}/pre-BCR^{+} ALL cells.

The combination therapy of dasatinib with ibrutinib reduces significantly CNS-infiltrating E2A-PBX1+/preBCR+ ALL after in vivo treatments.

Funding

This work was supported in part by grants of the German Research Foundation (DFG, DU 1287/5-1 to JDA), NIH (CA214888, to MLC), the William Lawrence and Blanche Hughes Foundation (to MLC). JDA and MLC received support of the Lucile Packard Foundation for Children's Health, the Child Health Research Institute and the Stanford NIH-NCATS-CTSA grant #UL1 TR001085. JDA also received support from the Berta Ottenstein-Programm for Advanced Clinician Scientists, Faculty of Medicine, University of Freiburg. JDA and MH received funding from ERA Per Med. JTC 2018 "GEPARD" project.

Corresponding Author:

Jesús Duque-Afonso

Department of Hematology/Oncology/Stem Cell Transplantation

Faculty of Medicine

University of Freiburg Medical Center

Hugstetterstr. 55

79106 Freiburg (Germany)

Email: jesus.duque.afonso@uniklinik-freiburg.de

Phone Number: +49 761 270 36000

Fax Number +49 761 270 72170

ORCID: 0000-0002-8287-5673

Data sharing statement

The data generated during and/or analyzed during the current study are available upon reasonable request from the corresponding author. The bulk RNA sequencing data has been deposited in Gene Expression Omnibus under the following accession number GSE221238, token clkhwucmttejpaf (http://ncbi.nlm.nih.gov/geo).

Conflict of Interests

The authors declare no potential conflict of interest with the submission of the abstract. J.D.-A. received speakers honoraria from Riemser, Lilly, Ipsen, Roche, Amgen, Beigene and AstraZeneca and travel support from Astra Zeneca, Ipsen, Gilead and Sobi. ML received research support from Janssen-Cilag.

Statement of significance:

In this work, we show promising preclinical *in vitro* and *in vivo* efficacy of combined targeted therapies with dasatinib and BTK inhibitors especially in the treatment of CNS-infiltrating E2A-PBX1+/preBCR+ ALL cells.

Title: 118 characters

Word abstract count: 204

Word count: 4799

Total number of figures and tables: 6

References: 44

Abstract

The t(1;19) translocation, which codes for the oncogenic fusion protein E2A (TCF3)-PBX1, is involved in acute lymphoblastic leukemia (ALL) and associated with a pre-B cell receptor (preBCR+) phenotype. Relapse in E2A-PBX1$^+$ ALL patients frequently occurs in the central nervous system (CNS). Therefore, there is a medical need for the identification of CNS active regimens for the treatment of E2A-PBX1$^+$/preBCR$^+$ ALL.

Using unbiased shRNA library screening approaches, we identified Bruton's tyrosine kinase (BTK) as a key gene involved in both proliferation and dasatinib sensitivity of E2A-PBX1$^+$/preBCR$^+$ ALL. Depletion of BTK by shRNAs resulted in decreased proliferation of dasatinib-treated E2A-PBX1$^+$/preBCR$^+$ cells compared with control-transduced cells. Moreover, combination of dasatinib with BTK inhibitors (BTKi) (ibrutinib, acalabrutinib or zanubrutinib) significantly decreased E2A-PBX1+/preBCR+ human and murine cell proliferation, reduced PLCG2 and BTK phosphorylation and total protein levels and increased disease-free survival of mice in secondary transplantation assays, reducing particularly CNS-leukemic infiltration. Hence, dasatinib with ibrutinib reduced pPLCG2 and pBTK in primary ALL patient samples, including E2A-PBX1$^+$ ALLs.

In summary, genetic depletion and pharmacological inhibition of BTK increase dasatinib effects in human and mouse E2A-PBX1$^+$/preBCR$^+$ ALL in most of performed assays, and the combination of dasatinib and BTKi is very effective in reducing CNS-infiltration of E2A-PBX1$^+$/preBCR$^+$ ALL cells in vivo.

Introduction

Acute lymphoblastic leukemia (ALL) is the most common cancer in children and is associated with poor prognosis in adults[1]. Even though the prognosis and treatment of ALL have significantly improved through intensified and stratified chemotherapy regimens[2], CNS relapse remains a major therapeutic obstacle to treat ALL. CNS involvement is observed in about 3-5% of patients at initial diagnosis and 30-40% of patients at relapse, including after allogeneic hematopoietic cell transplantation[3-5]. Therefore, a major clinical challenge in ALL is to identify and establish effective therapies in the context of CNS-infiltration by ALL cells.

ALL constitutes a family of genetically, morphologically, immunophenotypically and clinically heterogeneous lymphoid neoplasms derived from B- and T-lymphoid progenitors[6]. Among the B-ALL, a distinct immunophenotype characterized by expression and tonic functional activity of the pre-B cell receptor (preBCR) defines a novel ALL subtype (preBCR$^+$ ALL), accounting for 15% of ALL patients[7]. Half of preBCR$^+$ ALL cases harbor the chromosomal translocation t(1:19) (q23;p13), coding for the chimeric transcription factor E2A (TCF3)-PBX1 and affecting from 5 to 7 % of pediatric and adult ALL patients[8]. This genomic rearrangement fuses the transcription factor E2A (TCF3) with the homeobox gene PBX1[9] to serve as the initiating driver mutation in a phenotypically and genetically distinct subtype of ALL, which has also been associated with a higher incidence of CNS infiltration[10,11]. In E2A-PBX1$^+$ ALL, pathways downstream the preBCR are shown to be directly involved in CNS-infiltrating ALL cells and the *in vivo* CNS-infiltration of E2A-PBX1$^+$/preBCR$^+$ cells was observed in different mouse models[12-15].

In the last decades, several small-molecule inhibitors have shown *in vitro* and *in vivo* anti-tumor activity and their approval for clinical use as novel cancer treatments has drastically increased[16]. Dasatinib is an oral tyrosine kinase inhibitor (TKI), approved by the FDA as effective therapy in the treatment of chronic myeloid leukemia (CML) and

Philadelphia-chromosome-positive ALL (Ph^+ ALL)[17,18]. Recent studies have suggested dasatinib as a promising targeted therapy in other ALL subtypes, including $preBCR^+$ ALL[8,12,19-21]. Moreover, dasatinib has been described to cross the blood-brain barrier[22].

In this study, we aimed to identify novel targets to increase dasatinib efficacy, particularly with CNS activity, using genetic and pharmacological approaches. We identified and validated BTK as therapeutic target in murine models, human cell lines and human primary E2A-$PBX1^+$/$preBCR^+$ ALL, established combination therapies *in vitro* and *in vivo* of BTK inhibitors (BTKi) with dasatinib and demonstrated higher efficacy of the combination therapy in CNS-infiltrating E2A-$PBX1^+$/$preBCR^+$ ALL cells in *in vivo* transplantation models.

Materials and Methods

shRNA knockdown, lentiviral transfection, and competition growth assays

Individual *BTK-2* and *BTK-3* shRNA sequences (Suppl. Table S1) were cloned into the BstXI site of the p309 lentiviral vector, for stable transduction in human ALL cell lines[23,24]. The lentivirus generation was performed by co-transfection of shRNA constructs with pCMV-dR8.2 (packaging) and pCMV-VSVG (envelope) plasmids into HEK293T cells. Afterwards, human leukemia cells were transduced with viral supernatant, collected 48 h after transfection of HEK293T cells, using spinoculation (2500 rpm, 37 °C for 3 h) in the presence of 4 μg/ml polybrene. Cells were cultured for two days prior selection with 1 μg/ml puromycin (Invitrogen). After four days of selection, cells with control shRNAs (shLuc-mCherry) and shRNA knockdown for BTK (shBTK-2-mCherry, shBTK-3-mCherry) were mixed 1:1 with cells containing a control vector (shLuc-GFP), cultured for 24 days and monitored by flow cytometry for mCherry+ and GFP+ cells every 3 days. After puromycin selection, the knockdowns of the single shRNAs were confirmed by immunoblotting and quantitative RT-PCR.

Western blotting

Proteins were isolated using a modified radioimmunoprecipitation assay (RIPA) lysis buffer (50 mM Tris HCl, 1% NP-40, 1% natrium-deoxycholate, 150 mM NaCl, 1 mM EDTA, 1 mM PMSF, 1 mM Na3VO4), and 1x Protease inhibitor cocktail (Roche)[12]. Proteins were immunodetected with the following antibodies: rabbit anti-BTK (D3H5) (Cat. Nr. 8547; Cell signaling technology), rabbit anti-phospho-BTK (D9T6H) (Cat. Nr. 87141; Cell signaling technology), rabbit anti-PLCG2 (Cat. Nr. 3872; Cell signaling technology), rabbit anti-

phospho-PLCG2 (D9T6H) (Cat. Nr. 87141; Cell signaling technology), rabbit anti-GAPDH (14C10) (Cat. Nr. 2118; Cell signaling technology) antibodies.

qRT-PCR

The RNeasy Mini Kit (QIAGEN) was used to isolate the RNA, while the cDNA was synthesized using the SuperScript III Reverse Transcriptase Kit (Life Technologies) according to the manufacturer's recommendations. Relative expression of *BTK* (Hs04999593) gene and of *ACTB* (Hs01060665_g1) housekeeping gene were quantified using an LightCycler 480 II Thermocycler (Roche) with TaqMan gene expression assays from Thermo Fisher, and Light Cycler 480 Probes Master (Roche) at an annealing temperature of 60 °C.

Human cell lines

Human E2A-PBX1^{+}/preBCR^{+} (RCH-ACV and 697) cell lines and E2A-PBX1^{-} (REH and SEM) cell lines were cultured in RPMI 1640 medium supplemented with 10% FBS, 100 U/ml penicillin-streptomycin. B-ALL cell lines were authenticated in 2020 in DSMZ, after being obtained from DSMZ (Braunschweig, Germany) in 2013. Cell lines were negatively tested for Mycoplasma contamination by PCR. Human cell lines treated with vehicle (DMSO), dasatinib (BMS-354825), ibrutinib (PCI-32765), acalabrutinib (ACP-196), zanubrutinib (BGB-3111), from Selleck Chemicals (Houston, TX, USA), and with the combination of dasatinib with BTKis, at the indicated concentrations. Titration curves were performed using increasing drug concentrations and cells were counted by Trypan blue assay after 3 days.

Murine leukemia cells

Mouse leukemia E2A-PBX1^{+}/preBCR^{+} (#159) and E2A-PBX1^{+}/preBCR^{-} (#1496) cells (25,000/well) were cultured in methylcellulose medium (M3234, StemCell Technologies) supplemented with 10 ng/mL IL7 (Miltenyi Biotec). Leukemias cells were treated at the indicated concentrations in semi-solid methylcellulose medium (M3234, StemCell Technologies) supplemented with 10 ng/mL IL7 (Miltenyi Biotec). Titration curves were performed as described elsewhere[12].

Primary ALL samples

Primary ALL samples were obtained from Tissue bank of the University of Freiburg Medical School, Department of Hematology/Oncology, and primary E2A-PBX1^{+} ALLs from the tissue bank of the ALL BFM study group. Primary ALL samples were treated with vehicle (DMSO), dasatinib and ibrutinib from Selleck Chemicals (Houston, TX, USA), and with the combination of dasatinib with ibrutinib, at the indicated concentrations. Experiments with patient samples were performed in accordance with the tenets of the declaration of Helsinki and were approved by the Ethics Commission from the University of Freiburg (ethical vote, approval no. 279/17). All patients were informed by a physician and signed an informed consent form.

Antibodies and flow cytometry analysis

Phospho-flow and flow cytometry analysis were performed using standard conditions as described elsewhere[23]. For flow cytometry analysis the following antibodies were purchased: PLCG2- (K86-689.37) and BTK- (A3C6E2) Abs from BD Biosciences (Franklin Lakes, NJ, USA), 7-AAD-Ab (559925), CD34 (P28906) Abs from BD Pharmigen (San Diego, California, USA), CD45- (30-F11), CD19- (6D5), B220- (RA3-6B2), CD43- (S11) and CD117- (2B8) Abs from

Biolegend (San Diego, California, USA). The BD LSR Fortessa and FACS Aria III (BD Biosciences, Heidelberg, Germany) were used for analyzing and sorting.

Bone marrow transplantation assays

Secondary bone marrow transplantation using 1,000 murine E2A-PBX1^{+}/preBCR^{+} leukemia cells/recipient mouse, was performed after sublethal irradiation (6 Gy) of healthy recipient mice. Mice were treated i.p. (intraperitoneal injections) with: vehicle (30% PEG300, 5%Tween 80, 5% DMSO dissolved in PBS), dasatinib (5 mg/kg b.w./d), ibrutinib (20 mg/kg b.w./d), dasatinib in combination with ibrutinib (5 mg + 20 mg/kg b.w./d), acalabrutinib (20 mg/kg b.w./d), dasatinib in combination with acalabrutinib (5 mg + 20 mg/kg b.w./d), zanubrutinib (10 mg/kg b.w./d), dasatinib in combination with zanubrutinib (5 mg + 10 mg/kg b.w./d) from Selleck (Chemicals, Houston, TX, USA). Immunohistochemical analysis, cell blood counts, flow cytometry analysis for GFP+ cells and phospho-proteins and cell isolation for RNA sequencing and proteomics were performed after sacrificing animals with clinical signs of disease (lymphadenopathies, shivering or weakness) in order to analyze the efficacy of dasatinib and BTKi in an in vivo mouse transplantation model and identify mechanism of targeted therapy resistance. No animals were excluded from the analysis. No randomization method was used to allocate the animals to an experimental group. The investigators were not blinded to the group location during the experiment. All experiments were performed in accordance with relevant guidelines and regulations and were approved by the “Regierungspräsidium Freiburg“ (Nr. G-17/148).

Isolation of leukemia cells from CNS

Single cell suspensions were generated from fresh tissue from sacrificed mice. After isolation, both brain and spinal cord were cut in small pieces by scalpel and then were resuspended for 1h in the cell dissociation solution Accumax (Sigma-Aldrich, St Louis, MO, USA) at room temperature, followed by twice washing in PBS and GFP detection by flow cytometry.

Immunohistochemistry

Tissues were fixed in 10% formalin at 4°C overnight and embedded in paraffin[25]. Following dewaxing and antigen retrieval for 10 min at 96 °C in 0.1 M citrate buffer, incubation with polyclonal goat anti-GFP antibody (1:1000 dilution; Abcam, Cambridge, MA, USA, ab5450) was carried out overnight. Sections were incubated with biotin-conjugated anti-goat secondary antibody (1:200 dilution; Vector laboratories, Newark, CA, USA, BA-9500-1.5). Immunostatinings were quantified using QuPath (v.0.2.0) software that enables processing of digitalized images[26]. The images were transformed to DAB and GFP positivity was measured by pixel quantification by a single cut-off threshold of 0.20.

RNA sequencing and bioinformatics analysis

RNA from CNS of vehicle, dasatinib, ibrutinib, dasatinib + ibrutinib-treated mice was isolated using the RNeasy Plus Micro Kit (Qiagen) according to the manufacturer's instructions. RNA was used for RNAseq analysis following library preparation using the Illumina Stranded Total RNA Prep, Ligation with Ribo-Zero Plus kit.

Sequencing was performed in the Max-Planck-Institute für Immunbiology und Epigenetics using NovaSeq 6000. Sequencing data was processed using nf-core/rna-seq pipeline (version

3.8)[27]. Briefly, read quality was assessed by FastQC and MultiQC. Reads were trimmed to remove adapter sequences and poor-quality reads were removed with TrimGalore and ribosomal RNA was removed with SortMeRNA as preprocessing filtering tools. Filtered reads were then aligned to the Mouse genome (mm10) using STAR and read counts per gene were quantified using Salmon and post-processed with SAMtools and picard MarkDuplicates. In later steps, we used DESeq2 to remove genes with low counts keeping genes with at least 10 counts in a minimal number of samples (n=4). The differential gene expression analysis was performed with the limma + voom pipeline (v. 3.16)[28]. The significance threshold was set to adjusted p-value < 0.05.

Experiments with patient samples were approved by the Ethics Commission from the University of Freiburg (ethical vote, approval no. 279/17). All experiments with mice were performed in accordance with relevant guidelines and regulations and were approved by the "Regierungsprsidium Freiburg" (Nr. G-17/148).

Results

Identification of common genes and pathways involved in proliferation and dasatinib sensitivity using genetic screening approaches in E2A-PBX1$^+$ leukemia cells.

Functional genomic screens based on ultra-complex short hairpin RNA (shRNA) libraries were used in human E2A-PBX1$^+$ ALL cells to identify novel genes and pathways involved in cell proliferation and survival[23] and in dasatinib sensitivity and resistance[24]. Among the two previously performed shRNA screens, we identified 80 common genes from 3158 targeted genes, which significantly decreased cell proliferation and increased dasatinib sensitivity (Figure 1A, Suppl. Table S2). From the genes identified in both shRNA screens, we performed gene ontology analysis. Interestingly, the B-cell receptor (BCR) signaling pathway was enriched in both shRNA screens (Figure 1B). Only 6 genes were identified as common genes in both screens belonging to the BCR signaling pathway (*BTK*, *AKT2*, *MAP2K2*, *PIK3AP1*, *SYK* and *VAV*). In our previous work, we elucidated the role of PI3K/AKT/MTOR signaling pathway[23] and SYK[29] in E2A-PBX1$^+$/preBCR$^+$ ALL. Knowing the central role of BTK in the (pre)-BCR signaling pathway and the recent development of high potency BTKi with CNS activity, we focused our studies on this gene (Suppl. Table S1, Suppl. Figure S1).

BTK plays a key role in proliferation and survival as well as in dasatinib sensitivity in human E2A-PBX1$^+$/preBCR$^+$ ALL cells

Validation and functional characterization of the identified *BTK* gene was performed using a genetic shRNA-mediated knock-down approach followed by proliferation competition assays. Single shRNAs (sh-*BTK2* and sh-*BTK3*) were used to deplete efficiently *BTK* in human E2A-PBX1$^+$/preBCR$^+$ RCH-ACV cells using lentiviral vectors (Figure 1C-D, Suppl. Table S2). Stably transduced sh-Luc control cells and sh-*BTK2*/sh-*BTK3* knockdown cells were treated *in*

vitro with vehicle (DMSO) or TKI dasatinib (20 nM) for 24 days. Depletion of *BTK* by both shRNA constructs reduced the proliferation and survival, also in the presence of dasatinib, of transduced RCH-ACV cells compared to sh-Luc control transduced cells and to vehicle (DMSO) treated cells in competition assays (Figure 1E-F, Suppl. Figure S2), validating *BTK* as a key gene for cell proliferation/survival and dasatinib sensitivity in human E2A-PBX1$^+$/preBCR$^+$ ALL.

***In vitro* efficacy of pharmacologic targeted therapy with dasatinib in combination with BTK inhibitors in human E2A-PBX1$^+$/preBCR$^+$ ALL cells**.

To establish a combination therapy that increases dasatinib sensitivity especially in CNS in E2A-PBX1$^+$/preBCR$^+$ ALL, a pharmacologic approach was explored to test the effects of dasatinib in combination with the BTKi ibrutinib, which is known to penetrate the CNS very efficiently and has been established for the treatment of relapsed/refractory primary CNS-lymphoma[30,31] and CNS-infiltrating mantle cell lymphoma[32]. We hypothesized, that second generation BTKis (acalabrutinib and zanubrutinib) would also penetrate the CNS as ibrutinib and thus, were tested in combination with dasatinib. Indeed, clinical trials testing the efficacy of acalabrutinib in CNS-lymphoma are ongoing (NCT04548648).

First, we treated human RCH-ACV, 697, REH and SEM ALL cells with single substances and in combination. Dasatinib efficiently suppressed cell proliferation in E2A-PBX1$^+$/preBCR$^+$ RCH-ACV and 697 cell lines[29], with a dasatinib IC_{50} of 415 nM (RCH-ACV) and 247 nM (697), as previously shown (Suppl. Figure S3A). RCH-ACV and 697 showed similar sensitivity to BTKi, (IC50= 327 nM and 328 nM, respectively) as well as for acalabrutinib (IC50= 129 nM and 121 nM, respectively) and zanubrutinib (IC50= 220 nM and 193 nM, respectively) (Suppl. Figure S3B-D). Moreover, we observed a consistent statistically significant difference in sensitivity

to single treatments dasatinib and BTKis between human E2A-PBX1^{+}/preBCR^{+} and E2A-PBX1^{-}/preBCR^{-} cell lines (Suppl. Figure 3A-D). Furthermore, combination treatments with dasatinib and BTKis showed interactions at several concentrations as shown by the bliss index[33] on proliferation assays in human E2A-PBX1^{+}/preBCR^{+} RCH-ACV and 697 ALL cell lines (Figure 2A; Suppl. Figure S4A-B, S5A-B) but not in human E2A-PBX1^{-}/preBCR^{-} ALL SEM and REH cell lines at least at the selected concentrations (Suppl. Figure S6A-B). However, we cannot exclude negative, additive or synergistic effects at lower/higher concentrations in those cells. These data demonstrate that BTKis increase dasatinib sensitivity in human E2A-PBX1^{+}/preBCR^{+} but not in E2A-PBX1^{-}/preBCR^{-} ALLs, suggesting some selectivity.

Phosphorylation of PLCG2 and BTK decreases after combination therapy of dasatinib with BTKi in human E2A-PBX1^{+}/preBCR^{+} ALL cells.

Phospholipase C gamma2 (PLCG2) plays a critical role on BCR function and pPLCG2 is hyperactivated and has a pathogenic role in E2A-PBX1^{+}/preBCR^{+} ALL[29]. BTK is a key mediator of the (pre)-BCR pathway, upstream of PLCG2 and pBTK is increased after BCR signaling activation[34]. Therefore, we analyzed changes in phosphorylation status of pPLCG2 (Tyr 753) and pBTK (Tyr 223) using phospho-specific flow cytometry (phospho-flow) in ALL human cell lines after treatment with dasatinib in combination with BTKi. Treatments with single compounds reduced significantly pPLCG2 and pBTK in human E2A-PBX1^{+}/preBCR^{+} RCH-ACV and 697 ALL cell lines compared to vehicle treated cells. Combination treatments of dasatinib with BTK inhibitors further reduced pPLCG2 and pBTK compared to vehicle and single treatments (Figure 2B, Suppl. Figure S7A-C). As expected, human E2A-PBX1^{-}/preBCR^{-} SEM and REH ALL cell lines showed no significant differences in pPLCG2 and pBTK after treatment with single substances and dasatinib in combination with BTKi (Suppl. Figure S7A-

C). Moreover, the phosphorylation status of PLCG2 and BTK was assessed by Western blot. pPLCG2 was decreased after single treatments with dasatinib and BTKi. However, the combination of dasatinib and BTKi did not decrease further pPLCG2. In contrast, pBTK was slightly decreased after the combination of dasatinib and BTKi in human RCH-ACV ALL cell lines compared to the vehicle- and the single treatments. A decrease of total PLCG2 and BTK protein was also observed (Figure 2C). In summary, these data indicate that dasatinib and BTKis alone and in combination decrease phosphorylation and activation of key proteins PLCG2 and BTK involved in the preBCR signaling pathway.

BTK inhibition enhances *in vitro* efficacy of dasatinib in murine E2A-PBX1^{+}/preBCR^{+} but not in E2A-PBX1^{+}/preBCR^{-} ALL cells

To confirm that BTK inhibition enhances the effect of TKI dasatinib in E2A-PBX1^{+}/preBCR^{+} ALL cells, we followed a cross-species comparative approach using mouse ALL cell lines derived from our previously described conditioning E2A-PBX1 knock-in mouse model[29]. As previously shown, murine E2A-PBX1^{+}/preBCR^{+} #159 ALL cells were more sensitive to dasatinib and BTKi than murine E2A-PBX1^{+}/preBCR^{-} #1496 ALL cells (Suppl. Figure S8A-D). The IC_{50} of dasatinib was remarkably reduced in combination with BTKi at different concentrations in murine E2A-PBX1^{+}/preBCR^{+} #159 cells but not in E2A-PBX1^{+}/preBCR^{-} #1496 ALL cells (Suppl. Figure S9A-B). Similarly, to the human E2A-PBX1^{-}/preBCR^{-} ALL cell lines, we cannot exclude additive, synergistic or negative effects at higher or lower concentrations of the BTKis in murine E2A-PBX1^{+}/preBCR^{-} #1496 ALL cells.

We also analyzed the phosphorylation status of pPLCG2 and pBTK in murine ALL cell lines after the treatment with BTKis as monotherapies and in combination with dasatinib by phospho-flow. Combination therapies of BTKi with dasatinib reduced the pPLCG2 and pBTK

in murine E2A-PBX1^{+}/preBCR^{+} #159 but not E2A-PBX1^{+}/preBCR^{-} #1496 ALL cell lines compared to treatment with single substances and with vehicle-treated cells (Suppl. Figure S10A-B and S11). Western blot of murine E2A-PBX1^{+}/preBCR^{+} #159 ALL cells confirmed the decrease of pPLCG2 and pBTK and, similar to human E2A-PBX1^{+}/preBCR^{+} ALL cells and a decrease of total PLCG2 and BTK proteins after the treatment with single compounds and combination therapies was noted (Suppl. Figure S10B).

These data indicate that BTKis increase dasatinib effects on colony forming assays and reduction of PLCG2 and BTK phosphorylation in murine E2A-PBX1^{+}/preBCR^{+} but not in murine E2A-PBX1^{+}/preBCR^{-} ALLs, suggesting some selectivity for preBCR signaling inhibition.

***In vivo* efficacy of combination dasatinib and BTKi in E2A-PBX1^{+}/preBCR^{+} leukemias.**

To further validate and confirm the efficacy of the combination of dasatinib and BTKi, we analyzed *in vivo* treatments after transplantation of murine E2A-PBX1^{+}/preBCR^{+} ALL cells in sublethal irradiated healthy mouse recipients (Figure 3A). As expected, *in vivo* treatment with dasatinib in combination with BTKi, prolonged disease-free survival compared to vehicle- and single-treated mice (Figure 3B). The combination of dasatinib with BTKi reduced leukemia cell infiltration of several organs such as liver, spleen, lymph nodes as seen by hematoxylin and eosin (H&E) stainings and immunostainings by anti-GFP antibodies (Figure 3C; Suppl. Figure S12A-B). Mice treated with dasatinib combined with BTKi developed less lymphadenopathy, hepatomegaly and splenomegaly (Suppl. Figure S13A). Bone marrow insufficiency (anemia, thrombocytopenia), and leukocytosis were less pronounced in mice treated with the combination of dasatinib and BTKi (Suppl. Figure S13B). We showed presence of murine E2A-PBX1^{+}/preBCR^{+} leukemia cells in several organs by immunohistological stainings for GFP and we additionally quantified GFP+ leukemia cells by

flow cytometry. We confirmed that mice treated with the combination of dasatinib and BTKi showed less infiltration of GFP+ leukemia cells in analyzed organs and tissues (Figure 3C, Suppl. Figure S14-15).

Immunophenotypic analysis of GFP+ leukemia cells reveal significant differences on CD117 expression between E2A-PBX1+/preBCR+ #159 leukemia cells growth in vitro ($CD117^-$) and #159 leukemia cells derived from secondary transplantation experiments and in vivo treatments ($CD117^+$). We speculate that the change in CD117 expression between in vitro and in vivo cell growth might be explained by interactions of leukemic cells with microenvironment (i.e. presence of stem cell factor (SCF) in vivo and not in in vitro culture). No difference was found in the immunophenotype from leukemia cells derived from mice treated with dasatinib, ibrutinib or dasatinib + ibrutinib compared to vehicle-treated mice (Suppl. Figure S16).

Hence, we further validated the *in vivo* effect of dasatinib in combination with ibrutinib on total and phosphorylated PLCG2 and BTK proteins in bone marrow and spleen infiltrating E2A-$PBX1^+$/$preBCR^+$-GFP+ leukemic cells by phospho-flow. The infiltrating bone marrow and spleen GFP+ cells showed a significant decrease in both pPLCG2 (Tyr 753) and pBTK (Tyr 223) after the combination treatment compared to vehicle and single treatments after *in vivo* treatment with BTKis and dasatinib (Figure 3D, Suppl. Figure 17A-B). A significant decrease in total and phosphorylated BTK and PLCG2 proteins was detected in dasatinib+ibrutinib- compared to vehicle-treated murine E2A-PBX1+/preBCR+ ALL isolated from spleens from treated mice, similar to our *in vitro* experiments (Suppl. Figure 17A-B). These results confirmed the effect of BTKi and dasatinib on preBCR signaling pathway *in vivo* at the protein level

In vivo efficacy of combination treatment of dasatinib and BTKi on CNS-infiltrating murine E2A-PBX1^{+}/preBCR^{+} ALL cells.

As described previously, both dasatinib and BTKi can penetrate the blood–brain barrier, showing promising results in managing CNS-infiltrating leukemia and lymphomas[22, 30-32,35]. We hypothesized that the combination of dasatinib with BTKi may be more effective in reducing CNS-infiltrating ALL cells. We therefore immune-stained brain sections with anti-GFP antibody measuring GFP positivity by staining intensity in the immunohistochemistry. A significant reduction of GFP intensity from 15% in CNS samples of vehicle-treated to 3-5% in dasatinib-, ibrutinib- and dasatinib-ibrutinib-treated animals was observed (Figure 4A-B). Hence, we quantified the percentage of CNS infiltrating GFP+ leukemic cells by flow cytometry. Interestingly, GFP+ infiltrating leukemic cells were reduced to 4% in CNS in mice treated with dasatinib and ibrutinib, compared to the vehicle (mean 50%) or single treatments (about 20%), demonstrating superior efficacy of combination treatment for CNS-infiltrating leukemia cells (Figure 4C-E).

Transcriptomic analysis revealed crucial pathways for resistance in CNS-infiltrating E2A-PBX1^{+}/preBCR^{+} ALL cells.

In order to elucidate mechanism of resistance to BTKi and dasatinib in CNS-infiltrating leukemia cells and to investigate the CNS homing of E2A-PBX1/preBCR^{+} ALL cells, we performed global transcriptome analysis by RNA sequencing. Bioinformatics analysis identified 349 genes differentially regulated (159 up- and 190 downregulated, p-value <0.05) in the CNS-infiltrating leukemia cells after treatment with the combination of dasatinib with ibrutinib compared to vehicle-treated mice (Figure 5A-C, Suppl. Figure 18, Suppl. Table S3-6). Notably, the phosphatase and tensin homolog deleted on chromosome 10 (*Pten*) (log fold

change +0.86, p-value 0.044), the Mitogen-Activated Protein Kinase 1 (*Mapk1/Erk2*), (log fold change +0.43, p-value 0.043), and the proto-oncogene *Myc*, which play an important role in ALL, (log fold change -0.9, p-value 0.057) were subsequently validated by qPCR (Figure 5D). Other genes previously involved in the pathophysiology and CNS-infiltration in E2A-PBX1^{+}/preBCR^{+} as *Lck*, *Zap70* and *Cd79a*[13,15,29] showed a trend for decreased expression under the treatment with BTKi alone or in combination with dasatinib (Figure 5B).

***In vitro* efficacy of pharmacologic targeted therapy with dasatinib in combination with BTKi in primary ALL samples**.

To investigate the effect of the combination of dasatinib and BTKi in primary ALL samples, we performed phospho-flow assessing pPLCG2 (Tyr 753) and pBTK (Tyr 223) (Figure 6A). In gated CD19+ CD117+ blasts, the basal levels of pPLCG2 were relatively increased in t(11;12) and in two samples from patients with Burkitt lymphoma/leukemia compared to patients with c-ALL and pro-B-ALL. After treatment with dasatinib and ibrutinib, a significant decrease of pBTK and pPLCG2 in all samples was observed compared to vehicle-treated samples. In five primary pre-B-ALL E2A-PBX1^{+} t(1;19) samples we observed a slight decrease of pPLCG2 and a more significant decrease of pBTK after the combination treatment with dasatinib and ibrutinib (Figure 6B-C; Suppl. Figure 19).

Discussion

The cytoplasmic protein tyrosine kinase BTK is an essential component of the preBCR signaling pathway, on which lymphoid cells are dependent for development, proliferation and survival[34]. Several BTK inhibitors have shown antileukemic activity interfering with the mechanisms of malignant B-cell pathophysiology[36]. Treatments with BTK inhibitors or dasatinib have been shown to be effective in many different B cell malignancies[17-18,37-39].

Despite encouraging results and breakthrough treatments for ALL, CNS relapse of leukemia remains an unmet clinical need[10-11]. In this study, we investigated the role of BTK as key protein for proliferation and survival as well as BTK inhibition as a strategy to increase dasatinib sensitivity in E2A-PBX1$^+$/preBCR$^+$ ALL, particularly in CNS-infiltrating leukemia cells.

Although dasatinib has promising preclinical efficacy in the treatment of preBCR$^+$ ALL, including E2A-PBX1$^+$ leukemias[8,12,19-21], its efficacy is limited by the development of resistance *in vitro* and *in vivo*[24,29]. Using a shRNA library screening approach, targeting thousands of genes in human E2A-PBX1$^+$ leukemia cells[23,24], the BTK gene was identified by bioinformatic analysis as a key gene involved in dasatinib sensitivity and on which B-ALL cells are dependent for proliferation. We validated and confirmed the role of BTK as a regulator of proliferation and increasing dasatinib sensitivity of E2A-PBX1$^+$/preBCR$^+$ RCH-ACV cells by competition assays after single shRNA knock-down assays.

Aiming to improve the efficacy of the treatment of CNS-infiltrating E2A-PBX1$^+$/preBCR$^+$ ALL cells, we took advantage of the pharmacological properties of dasatinib and BTKis (ibrutinib, acalabrutinib and zanubrutinib) to cross the blood-brain barrier and establish combination therapies, which are very effective for the treatment of systemic but also CNS-infiltrating disease.

Due to the oncogenic role of BTK in B-cell malignancies, several BTKi have been developed over time are currently approved for patient treatment[37-39]. In this study, we

particularly focused our attention on the BTKi ibrutinib, acalabrutinib and zanubrutinib. Ibrutinib is a selective and irreversible inhibitor of BTK, and a promising therapeutic option for preBCR$^+$ or TCF3-rearranged ALL[21]. Acalabrutinib and zanubrutinib are potent BTKi, with improved selectivity and lower off-target effects in comparison with ibrutinib[40,41].

As expected, the *in vitro* combination of dasatinib with BTKi displayed at least an additive anti-proliferative effect on E2A-PBX1$^+$/preBCR$^+$ human RCH-ACV and 697 cells and murine #159 cells. In addition, the combination therapies led to an *in vitro* decrease of PLCG2 and BTK expression levels and affected also the phosphorylation status of PLCG2 and BTK, reduced in human and murine E2A-PBX1$^+$/preBCR$^+$ cell lines and in the spleen-infiltrating ALL cells. Our findings imply that the pharmacological combinations of dasatinib and BTKi cause a high impact on B-cell growth and confirmed BTK as a key regulator of dasatinib sensitivity *in vitro*.

In addition, using a secondary transplanted E2A-PBX1$^+$ ALL mouse model as a preclinical platform, we validated the therapeutic *in vivo* efficacy of dasatinib in combination with BTKis. We observed a statistically significant prolonged disease-free survival of mice treated with dasatinib- combined with BTKi, implying that the combination therapies might have clinical efficacy in the treatment of a subset of preB-ALL. Of note, changes in levels and distribution of E2A-PBX1$^+$/preBCR$^+$ GFP+ infiltrating leukemia cells were visualized in several organs, including the CNS by immunohistochemistry and flow cytometry, in which the combined treatment therapy drastically decreased the percentage of tumor-infiltrating cells. Of note, treatment with BTKi and dasatinib was limited on time (20 days) and we used a single dose proven to be effective. Mice receiving the combined treatment start getting sick and showing CNS infiltrating ALL cells beyond this period of time. We suggest that continuous treatment with the combination therapy till disease progress or relapse and

assessment of maximal tolerated dose in single and combination treatments might improve the clinical efficacy in future clinical trials.

Due to short time between treatment stop and leukemia development in dasatinib and BTKi-treated mice, we hypothesize that dasatinib and BTKi treatments were able to inhibit efficiently leukemia cell proliferation as long as the treatments were given. Nevertheless, resistant and/or very aggressive leukemic subclones might have been already present under the treatment and might have expanded very quickly after treatment withdrawal. However, we did not confirm dasatinib- and BTKi-resistance in *in vitro* experiments in leukemia cells from sacrificed mice. These data suggest a continuous treatment with dasatinib and BTKi as effective schedule for possible future clinical trials in human ALL.

Our results show that the combination therapy of dasatinib and BTKis has a drastic impact on CNS-infiltrating E2A-PBX1^{+}/preBCR^{+} leukemia cells in our mouse model. These data are consistent with the above-discussed *in vitro* efficacy of the combined therapies on overcoming the dasatinib resistance in E2A-PBX1^{+}/preBCR^{+} ALL[29], highlighting the impact on CNS-infiltrating leukemic cells.

Moreover, the data from the RNA sequencing analysis showed that the tumor suppressor *Pten*, which plays a key role in development and maintenance of CNS[42] and chemotherapy resistance in T-ALL[43], is upregulated in the CNS of vehicle-treated mice compared to mice treated with dasatinib+ibrutinib. The upregulation of *Mapk1/Erk2*, whose signaling is involved in CNS-ALL cells survival, in the double treated- compared to vehicle-treated mice may be the result of therapy resistant mechanism, in which the inhibition of preBCR signaling pathway by dasatinib and ibrutinib leads to alternative activation of MAPK signaling pathway[44]. The proto-oncogene Myc is instead downregulated in CNS after the

double treatment compared to vehicle treatment, suggesting effective inhibition of this oncogenic signaling pathway in CNS-infiltrating cells. We speculate, that E2A-PBX1^{+}/preBCR^{+} ALL cells resistant to combined treatment with BTKi+dasatinib arising in CNS are dependent on alternative pathways as MAPK signaling pathways, which might be targeted by small molecule inhibitors as MEK inhibitors.

One of our goals in this study was not only to analyze global transcriptional changes at the mRNA level but also at protein level. The results of our in vitro/in vivo analysis assessed by western blots and phospho-specific flow cytometry, indicated a decrease not only on phosphorylated but also on total proteins involved in the preBCR signaling pathway as BTK and PLCG2 under treatment with BTKi and dasatinib.

Furthermore, the combination of dasatinib and BTKi shows also activity on reducing pBTK and pPLCG2 in primary ALL with different karyotypes including E2A-PBX1^{+}/preBCR^{+} ALL, suggesting therapeutic activity of this combination therapy beyond E2A-PBX1^{+}/preBCR^{+} ALL. In summary, our findings demonstrate promising preclinical *in vitro* and *in vivo* efficacy of dasatinib and BTKi, especially in CNS-infiltrating ALL cells, using mouse, human cell lines and human primary E2A-PBX1^{+}/preBCR^{+} ALL.

Acknowledgements

We would like to acknowledge the Lighthouse Core Facility for their assistance with FACS analysis and qPCR assays, all members of the Duque lab for assistance and helpful comments. The authors wish to acknowledge UEF Bioinformatics Center, University of Eastern Finland, Finland for computational resources. We thank C. Duque-Afonso for graphic design.

Author Contributions

GG planned and performed the experiments. JD-A designed the experiments. GG and TP performed mouse experiments. GG and AC performed immunohistochemical stainings. MP, DWM and RS prepared the paraffin-embedded mice samples blocks. MLü and TM provided reagents. GG and TM prepared the RNA samples for sequencing. MH, MLa and MV analyzed the RNA sequencing data. GG and MAM performed the phospho-specific flow cytometry (phospho-flow). GG and TP performed the phospho-flow on primary samples. MCB, KH and DWM designed, performed and analyzed the data from shRNA library screen assay. LL, GC, MS, MS and JDu provided patient samples. MLC provided mouse E2A-PBX1^{+} leukemia cells. GG and JD-A wrote the manuscript and prepared the figures. GG and J.D-A. analyzed the data of primary ALL and all authors have access to clinical data. All authors revised the final version of the paper. All authors have read and agreed to the published version of the manuscript.

Conflict of Interests

The authors declare no potential conflict of interest with the submission of the abstract. J.D.-A. received speakers honoraria from Riemser, Lilly, Ipsen, Roche, Amgen and AstraZeneca and travel support from Astra Zeneca, Ipsen, Gilead and Sobi.

Funding

This work was supported in part by grants of the German Research Foundation (DFG, DU 1287/5-1 to JDA), NIH (CA214888, to MLC), the William Lawrence and Blanche Hughes Foundation (to MLC). JDA and MLC received support of the Lucile Packard Foundation for Children's Health, the Child Health Research Institute and the Stanford NIH-NCATS-CTSA grant #UL1 TR001085. JDA also received support from the Berta Ottenstein-Programm for Advanced Clinician Scientists, Faculty of Medicine, University of Freiburg. JDA and MH received funding from ERA Per Med. JTC 2018 "GEPARD" project.

Study approval

Experiments with patient samples were approved by the Ethics Commission from the University of Freiburg (ethical vote, approval no. 279/17). All experiments with mice were performed in accordance with relevant guidelines and regulations and were approved by the "Regierungspräsidium Freiburg" (Nr. G-17/148).

Supplementary material

This article includes supplementary material.

References

1. Erdmann F, Spix C, Schrappe M, Borkhardt A, Schüz J. Temporal changes of the incidence of childhood cancer in Germany during the COVID-19 pandemic: Updated analyses from the German Childhood Cancer Registry. *Lancet Reg Health Eur*. **2022**; 17: 100398

2. Gökbuget N, Stanze D, Beck J, Diedrich H, Horst HA, Hüttmann A, *et al*. Outcome of relapsed adult lymphoblastic leukemia depends on response to salvage chemotherapy, prognostic factors, and performance of stem cell transplantation. *Blood* **2012**; 120: 2032–2041.

3. Lenk L, Alsadeq A, Schewe DM. Involvement of the central nervous system in acute lymphoblastic leukemia: opinions on molecular mechanisms and clinical implications based on recent data. *Cancer Metastasis Rev*. **2020**; 39: 173–187.

4. Pui CH & Howard SC. Current management and challenges of malignant disease in the CNS in paediatric leukaemia. *Lancet Oncol*. **2008**; 9: 257–268.

5. Kharfan-Dabaja MA, Labopin M, Bazarbachi A, Salmenniemi U, Mielke S, Chevallier P, *et al.* CNS Involvement at Initial Diagnosis and Risk of Relapse After Allogeneic HCT for Acute Lymphoblastic. *Hemasphere* **2022**; 6: e788.

6. Inaba H, Pui CH. Advances in the diagnosis and treatment of pediatric acute lymphoblastic leukemia. *J. Clin. Med.* **2021**; 10: 1926

7. Köhrer S, Havranek O, Seyfried F, Hurtz C, Coffey GP, Kim E, *et al*. Pre-BCR signaling in precursor B-cell acute lymphoblastic leukemia regulates PI3K/AKT, FOXO1 and MYC, and can be targeted by SYK inhibition. *Leukemia* **2016**; 30: 1246-54.

8. Geng H, Hurtz C, Lenz KB, Chen Z, Baumjohann D, Thompson S, *et al*. Self-enforcing feedback activation between BCL6 and pre-B cell receptor signaling defines a distinct subtype of acute lymphoblastic leukemia. *Cancer Cell* **2015**; 27: 409-25.

9. Hunger SP, Galili N, Carroll AJ, Crist WM, Link MP, Cleary ML. The t(1;19)(q23;p13) results in consistent fusion of E2A and PBX1 coding sequences in acute lymphoblastic leukemias. *Blood* **1991**; 77: 687-93.

10. Jeha S, Pei D, Raimondi SC, Onciu M, Campana D, Cheng C, *et al*. Increased risk for CNS relapse in pre-B cell leukemia with the t(1;19)/TCF3-PBX1. *Leukemia* **2009**; 23: 1406–1409.

11. Sanchez R, Ayala R, Alonso RA, Martínez MP, Ribera J, García O, *et al.* Clinical characteristics of patients with central nervous system relapse in BCR-ABL1-positive acute lymphoblastic leukemia: The importance of characterizing ABL1 mutations in cerebrospinal fluid. *Annals of Hematology* **2017**; 96: 1069–1075.

12. Duque-Afonso J, Feng J, Scherer F, Lin CH, Wong SH, Wang Z, *et al.* Comparative genomics reveals multistep pathogenesis of E2A-PBX1 acute lymphoblastic leukemia. *The Journal of Clinical Investigation* **2015**; 125: 3667–3680.

13. Alsadeq A, Fedders H, Vokuhl C, Belau NM, Zimmermann M, Wirbelauer T, *et al*. The role of ZAP70 kinase in acute lymphoblastic leukemia infiltration into the central nervous system. *Haematologica* **2017**; 102: 346–355.

14. Krause S, Pfeiffer C, Strube S, Alsadeq A, Fedders H, Vokuhl C, *et al*. Mer tyrosine kinase promotes the survival of t(1;19)-positive acute lymphoblastic leukemia (ALL) in the central nervous system (CNS). *Blood* **2015**; 125: 820–830.

15. Lenk L, Carlet M, Vogiatzi F, Spory L, Winterberg D, Cousins A, *et al*. CD79a promotes CNS-infiltration and leukemia engraftment in pediatric B-cell precursor acute lymphoblastic leukemia. *Commun Biol.* **2021**; 4: 73.

16. Roskoski R. Properties of FDA-approved small molecule protein kinase inhibitors: A 2021 update. *Pharmacological Research*. **2021**.

17. Kantarjian H, Shah NP, Hochhaus A, Cortes J, Shah S, Ayala M, *et al.* Dasatinib versus imatinib in newly diagnosed chronic-phase chronic myeloid leukemia. *N Engl J Med.* **2010**; 362: 2260-70.

18. Foà R, Vitale A, Vignetti M, Meloni G, Guarini A, De Propris MS, *et al.* Dasatinib as first-line treatment for adult patients with Philadelphia chromosome-positive acute lymphoblastic leukemia. *Blood* **2011**; 118: 6521-8.

19. Bicocca VT, Chang BH, Masouleh BK, Muschen M, Loriaux MM, Druker BJ, *et al.* Crosstalk between ROR1 and the Pre-B cell receptor promotes survival of t(1;19) acute lymphoblastic leukemia. *Cancer Cell* **2012**; 22: 656-67.

20. Eldfors S, Kuusanmäki H, Kontro M, Majumder MM, Parsons A, Edgren H, *et al.* Idelalisib sensitivity and mechanisms of disease progression in relapsed TCF3-PBX1 acute lymphoblastic leukemia. *Leukemia* **2017**; 31: 51-57.

21. Fischer U, Forster M, Rinaldi A, Risch T, Sungalee S, Warnatz HJ, *et al.* Genomics and drug profiling of fatal TCF3-HLF-positive acute lymphoblastic leukemia identifies recurrent mutation patterns and therapeutic options. *Nat Genet.* **2015**; 47: 1020-1029.

22. Porkka K, Koskenvesa P, Lundan T, Rimpiläinen J, Mustjoki S, Smykla R, *et al.* Dasatinib crosses the blood-brain barrier and is an efficient therapy for central nervous system Philadelphia chromosome–positive leukemia. *Blood* **2008**; 112: 1005–1012.

23. Grüninger PK, Uhl F, Herzog H, Gentile G, Andrade-Martinez M, Schmidt T, *et al.* Functional characterization of the PI3K/AKT/MTOR signaling pathway for targeted therapy in B-precursor acute lymphoblastic leukemia. *Cancer Gene Ther.* **2022**; 29: 1751-1760.

24. Duque-Afonso J, Lin CH, Han K, Morgens DW, Jeng EE, Weng Z, *et al.* CBP Modulates Sensitivity to Dasatinib in Pre-BCR+ Acute Lymphoblastic Leukemia. *Cancer Res.* **2018**; 78: 6497-6508.

25. Catalano A, Adlesic M, Kaltenbacher T, Klar RFU, Albers J, Seidel P, *et al.* Sensitivity and Resistance of Oncogenic RAS-Driven Tumors to Dual MEK and ERK Inhibition. *Cancers (Basel)* **2021**; 13: 1852.

26. Bankhead P, Loughrey MB, Fernández JA, Dombrowski Y, McArt DG, Dunne PD, McQuaid S, Gray RT, Murray LJ, Coleman HG, James JA, Salto-Tellez M, Hamilton PW. QuPath: Open source software for digital pathology image analysis. *Sci Rep.* **2017**; 7**:** 16878.

27. Ewels PA, Peltzer A, Fillinger S, Patel H, Alneberg J, Wilm A, *et al.* The nf-core framework for community-curated bioinformatics pipeline. *Nat. Biotechnol.* **2020**; 38: 276-278

28. Ritchie ME, Phipson B, Wu D, Hu Y, Law CW, Shi W, *et al.* limma powers differential expression analysis for RNA-sequencing and microarray studies. *Nucleic Acids Res.* **2015**; 43: e47

29. Duque-Afonso J, Lin CH, Han K, Morgens DW, Jeng EE, Weng Z, *et al.* E2A-PBX1 Remodels Oncogenic Signaling Networks in B-cell Precursor Acute Lymphoid Leukemia. *Cancer Res.* **2016**; 76: 6937-6949.

30. Soussain C, Choquet S, Blonski M, Leclercq D, Houillier C, Rezai K, *et al.* Ibrutinib monotherapy for relapse or refractory primary CNS lymphoma and primary vitreoretinal lymphoma: final analysis of the phase II 'proof-of-concept' iLOC study by the Lymphoma study association (LYSA) and the French oculo-cerebral lymphoma (LOC) net. *Eur. J. Cancer* **2019**; 117: 121–30.

31. Lauer EM, Waterhouse M, Braig M, Mutter J, Bleul S, Duque-Afonso J, *et al.* Ibrutinib in patients with relapsed/refractory central nervous system lymphoma: A retrospective single-centre analysis. *Br. J. Haematol* **2020**; 190: e110-e114.

32. Rusconi C, Cheah CY, Eyre TA, Tucker D, Klener P, Giné E, *et al.* Ibrutinib improves survival compared with chemotherapy in mantle cell lymphoma with central nervous system relapse. *Blood* **2022**; 140: 1907-1916.

33 Bliss CI. The calculation of microbial assays. Bacteriol Rev. 1956;20:243–58.

34. Kim E, Hurtz C, Koehrer S, Wang Z, Balasubramanian S, Chang BY, *et al.* Ibrutinib inhibits pre-BCR$^+$ B-cell acute lymphoblastic leukemia progression by targeting BTK and BLK. *Blood* **2017**; 129: 1155-1165.

35. Krishnan S, Wade R, Moorman AV, Mitchell C, Kinsey SE, Eden TO, *et al.* Temporal changes in the incidence and pattern of central nervous system relapses in children with acute lymphoblastic leukaemia treated on four consecutive Medical Research Council trials, 1985-2001. *Leukemia* **2010**; 24: 450-9.

36. Estupiñán HY, Wang Q, Berglöf A, Schaafsma GCP, Shi Y, Zhou L, *et al.* BTK gatekeeper residue variation combined with cysteine 481 substitution causes super-resistance to irreversible inhibitors acalabrutinib, ibrutinib and zanubrutinib. *Leukemia* **2021**; 35: 1317-1329.

37. Burger JA, Tedeschi A, Barr PM, Robak T, Owen C, Ghia P, *et al.* Ibrutinib as Initial Therapy for Patients with Chronic Lymphocytic Leukemia. *N Engl J Med.* **2015**; 373: 2425-37.

38. Tam CS, Dimopoulos M, Garcia-Sanz R, Trotman J, Opat S, Roberts AW, *et al.* Pooled safety analysis of zanubrutinib monotherapy in patients with B-cell malignancies. Blood Adv. **2022**; 6: 1296-1308.

39. Byrd JC, Hillmen P, Ghia P, Kater AP, Chanan-Khan A, Furman RR, *et al.* Acalabrutinib Versus Ibrutinib in Previously Treated Chronic Lymphocytic Leukemia: Results of the First Randomized Phase III Trial. *J. Clin. Oncol.* **2021**; 39: 3441-3452.

40. Barf T, Covey T, Izumi R, van de Kar B, Gulrajani M, van Lith B, *et al.* Acalabrutinib (ACP-196): A Covalent Bruton Tyrosine Kinase Inhibitor with a Differentiated Selectivity and In Vivo Potency Profile. *J. Pharmacol. Exp. Ther.* **2017**; 363: 240-252.

41. Guo Y, Liu Y, Hu N, Yu D, Zhou C, Shi G, *et al.* Discovery of Zanubrutinib (BGB-3111), a novel, potent, and selective covalent inhibitor of Bruton's tyrosine kinase. *J. Med. Chem.* **2019**; 62: 7923–40.

42. Zou H, Ding Y, Shi W, Xu X, Gong A, Zhang Z, *et al.* MicroRNA-29c/PTEN pathway is involved in mice brain development and modulates neurite outgrowth in PC12 cells. *Cell. Mol. Neurobiol.* **2015**; 35: 313-322.

43. Hlozkova K, Hermanova I, Safrhansova L, Alquezar-Artieda N, Kuzilkova D, Vavrova A, *et al.* PTEN/PI3K/Akt pathway alters sensitivity of T-cell acute lymphoblastic leukemia to L-asparaginase. *Sci. Rep.* **2022***;* 12: 4043.

44. Packer LM, Rana S, Hayward R, O' Hare T, Eide CA, Rebocho A, et al. Nilotinib and MEK inhibitors induce synthetic lethality through paradoxical activation of RAF in drug-resistant chronic myeloid leukemia. *Cancer Cell* **2011**; 20: 715-27.

Figures and Figure legends

Figure 1 BTK-depletion decreases the proliferation of human E2A-PBX1$^+$/preBCR$^+$ RCH-ACV cells treated with dasatinib. (A) Using a shRNA library screen approach, the Bruton's tyrosine kinase (BTK) was identified as key gene involved to increase sensitivity to dasatinib in E2A-PBX1$^+$/preBCR$^+$ leukemia cells. **(B)** Gene ontology analysis of pathways enriched in genes increasing sensitivity to dasatinib. Only the top 10 KEGG pathways are showed. **(C)** RT-qPCR shows efficient shRNA-mediated knockdown of *BTK2* and *BTK3*. **(D)** Western blot analysis (representative of three independent experiments) shows the protein levels following knockdown by sh-BTK2 and sh-BTK3 constructs in RCH-ACV cells. mRNA and protein were extracted from the same stably transduced expanded sh-Luc control cells and sh-BTK2/sh-BTK3 knockdown cells used for (C) and (D) experiments. GADPH was used as loading control. Densitometry values were calculated using ImageJ software. **(E)** Graph shows the percentage of mCherry$^+$ cells transduced with shRNAs for luciferase (control) or shRNA constructs of BTK2 or BTK3 and treated with dasatinib 20 nM for 24 days. Data represent the mean ± SEM of three independent experiments. Statistical analysis performed by non-parametric Mann Whitney test. n.s., not significant; ***, $p<0.001$. **(F)** Dot plot proportion of mCherry+ and GFP+ cells in flow cytometry at day 24 of culture of a representative experiment, in which RCH-ACV cells were transduced with control shRNA (shLuc, Luciferase) or shRNA for BTK (shBTK2 and shBTK3) with a mCherry as fluorescence marker.

Figure 2. In vitro effect of combined therapy with dasatinib and BTK inhibitors on human E2A-PBX1$^+$/preBCR$^+$ ALL cell proliferation and on PLCG2 and BTK phosphorylation. **(A)** *Left panels,* titration curves for E2A-PBX1$^+$ /preBCR$^+$ human (RCH-ACV) cells with increasing concentrations of dasatinib and ibrutinib combination treatments. Viable RCH-ACV cells were counted with trypan blue exclusion assay after 3 days. Data represent IC_{50} calculated using non-linear regression analysis and curves were compared with the sum-of-squares F test. Dose-response curves of each BTKi concentration were compared to the dose-response curve of the vehicle-treated cells as controls. ns not significant; **, $p < 0.001$; ***, $p < 0.0001$. *Right panel*, heatmap representation of Bliss interaction index for RCH-ACV cells treated with dasatinib and ibrutinib. Three independent experiments were performed. **(B)** *In vitro* effects of the combined therapy with dasatinib and BTK inhibitors in human RCH-ACV cells on the phosphorylation status of the key pre-BCR$^+$ pathway proteins PLCG2 and BTK, after 30 min of treatment. One representative graph per antibody is showed. Relative fold median fluorescence intensity (MFI) change of cells treated with inhibitors or vehicle are illustrated. Data represent mean of three independent experiments + SEM. **(C)** Western blot analysis (representative of three independent experiments) shows the protein levels of BTK, pBTK, PLCG2 and pPLCG2 following dasatinib (1 nM), ibrutinib (100 nM), dasatinib (1 nM) + ibrutinib (100 nM) treatments compared to control, in human RCH-ACV ALL cells. GADPH was used as loading control. Densitometry values were calculated using ImageJ software.

Figure 3. *In vivo* sensitivity of E2A-PBX1$^+$/preBCR$^+$ leukemia cells to the combination of dasatinib and BTKi. **(A)** Schematic representation of secondary transplantations of E2A-PBX1$^+$/preBCR$^+$ leukemia cells in healthy recipients and in vivo treatment with vehicle, dasatinib, BTKis and combination of dasatinib with BTKis. **(B)** E2A-PBX1$^+$ leukemia cells from preBCR$^+$ leukemia were transplanted into sublethally irradiated recipient healthy C57/BL6 mice. Mice were treated for 20 days with vehicle (n=10), dasatinib (n=10), ibrutinib (n=10), dasatinib + ibrutinib (n=10), acalabrutinib (n=5), dasatinib + acalabrutinib (n=5), zanubrutinib (n=5), dasatinib + zanubrutinib (n=5). *In vivo* dasatinib+BTKi treatments of pre-BCR$^+$ leukemia in a secondary transplantation assay led to significantly prolonged disease-free survival compared to vehicle-treated mice. Statistical analysis was performed by log-rank test. **(C)** Immunohistochemical staining of bone marrow (BM) sections with anti-GFP antibody showing a decrease in GFP$^+$ E2A-PBX1$^+$/pre-BCR$^+$ leukemic cells infiltration in double treated mice compared to single- and vehicle-treated mice. Samples were collected from sacrificed animals with signs of disease from vehicle- (mean = 18 days), dasatinib (mean= 24 days), ibrutinib (mean = 30 days), dasatinib + ibrutinib (mean = 37 days) treated animals. Objective lens: 20×; Scale bar: 200 µm. GFP positivity was measured using the QuPath software after transformation of images to DAB and staining intensity quantified by a single cut-off threshold of 0.20. **(D)** The phosphorylation status of p-PLCG2 (Tyr 753) and p-BTK (Tyr 223) of bone marrow murine cells by phospho-specific flow cytometry. The phosphorylation of both PLCG2 and BTK decrease significantly in the bone marrow isolated from dasatinib + ibrutinib treated mice. Fold median fluorescence intensity (MFI) change of dasatinib, ibrutinib and dasatinib + ibrutinib treated mice compared to vehicle. Data represent mean of three independent experiments + SEM. BM, bone marrow. * $p < 0.01$; ** $p < 0.001$; ***, $p < 0.0001$; n.s., not significant.

Figure 4. Decrease of CNS infiltration of leukemia cells by combination therapy with dasatinib and BTKi. (A) *Upper panels,* images of mouse brain rostral leptomeninges slices from wild type C57/BL6 mice, vehicle, dasatinib, ibrutinib and dasatinib + ibrutinib treated mice tissues, stained using the H&E method. Vehicle-treated mice show an increased level of leukemic infiltration (arrow) compared to the dasatinib, ibrutinib and dasatinib + ibrutinib treated mice. Samples were collected from sacrificed animals with signs of disease from vehicle- (mean = 18 days), dasatinib (mean= 24 days), ibrutinib (mean = 30 days), dasatinib + ibrutinib (mean = 37 days) treated animals. Objective lens: 40×; Scale bar: 50 µm. *Lower panels,* immunohistochemical staining of CNS sections with anti-GFP antibody showing less GFP^+ E2A-$PBX1^+$/$preBCR^+$ leukemic cells infiltration in double- and single-treated mice compared to vehicle-treated mice. Arrows pointing at leukemic CNS infiltration. Unstained CNS sections are showed. Objective lens: 20×; Scale bar: 200 µm. **(B)** GFP positivity from 3 representative mice of each group was estimated after transformation of images to DAB and GFP staining intensity quantified by a single cut-off threshold of 0.20. Statistical analysis was performed by one-way ANOVA, Dunnett's Multiple Comparison Test. **(C)** Single cell suspensions from fresh tissue from both brain and spinal cord after cutting in small pieces by scalpel and resuspended in a cell dissociation solution were used for quantification of GFP+ cells in flow cytometry. Panels show the gating strategy for phospho-flow cytometry staining for GFP^+ murine E2A-PBX1+/pre-BCR+ leukemia cells from vehicle, dasatinib, ibrutinib and dasatinib + ibrutinib treated mice. Gating was performed on lymphocytes, single cells, and GFP^+ cells. The frequency of GFP^+ murine E2A-$PBX1^+$/$preBCR^+$ leukemia cells decrease in the combination treatment. **(D, E)** Frequency of GFP^+ murine leukemia infiltrating **(D)** the brain and **(E)** the spinal cord of C57BL/6 wt, mice. Each symbol represents an individual mouse. Statistical analysis was performed by one-way ANOVA, Dunnett's Multiple Comparison Test. Scatter dot plots represent mean ± SEM. **, $p<0.01$; ***, $p < 0.0001$. IHC, immunehistochemistry.

Figure 5. RNAseq of E2A-PBX1^{+}/preBCR^{+} leukemia CNS infiltrating cells compared across treatments. Bulk RNAseq of FACS-sorted CNS-infiltration E2A-PBX1-GFP+ leukemic cells from vehicle- (n=3), dasatinib- (n=3), ibrutinib- (n=3) and dasatinib+ibrutinib-treated mice (n=3) was performed. **(A)** MA plot displaying 349 most significant genes (p value < 0.05) between all the treatments. **(B)** Heatmap showing B-cell receptor associated differential expressed (DE) genes. *Myc* (p-value 0.06) is downregulated in the double-treated mice compared to vehicle-treated mice. A trend for decreased expression of BCR-associated genes *Lck, Zap70* and *Cd79a* showed a trend for decreased expression under the treatment with BTKi alone or in combination with dasatinib. In contrast, *Pten* (p-value<0.05) and *Mapk1/ERK2* (p-value<0.05) are upregulated in the double-treated mice compared to vehicle-treated mice. **(C)** Venn diagrams showing the most significant in-common up- and downregulated genes between the treatments. **(D)** Validation of *Pten*, *Myc* and *Mapk1* genes by RT-qPCR. *Actb* was used as house keeping gene. The experiment was performed in triplicate. Bars represent the mean and error bars, the SEM, of 3 independent experiments.

Figure 6. *In vitro* effect of combined therapy with dasatinib and BTKi on primary ALL samples. (A) Flow cytometric analysis of primary samples aiming to detect the phosphorylation status of PLCG2 and BTK after 30 min of treatment with vehicle (DMSO), dasatinib, ibrutinib, dasatinib + ibrutinib. Gating strategy on lymphocytes, single cells, 7AAD, CD19+ CD117+. One representative histogram per antibody is showed. **(B-C)** Histogram represents the phosphorylation of **(B)** PLCG2 and **(C)** BTK in primary ALL samples with different karyotypes, after treatment with vehicle, ibrutinib, dasatinib and dasatinib + ibrutinib treatment.

Figure 1 BTK-depletion decreases the proliferation of human E2A-PBX1+/preBCR+ RCH-ACV cell treated with dasatinib

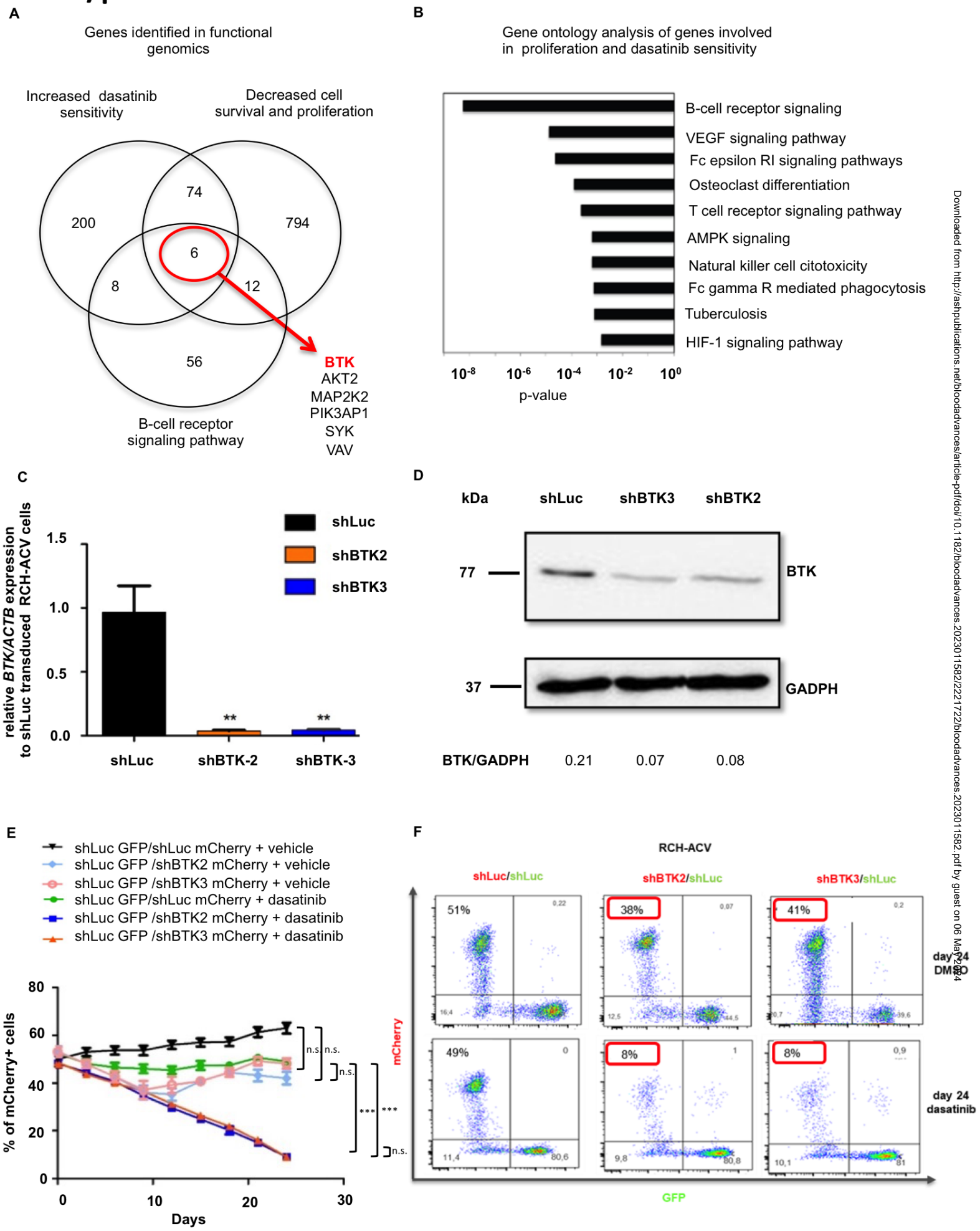

Figure 2

Figure 2. *In vitro* effect of combined therapy with dasatinib and BTK inhibitors on human B-ALL E2A-PBX1⁺/preBCR⁺ cells proliferation and on PLCG2 and BTK phosphorylation status.

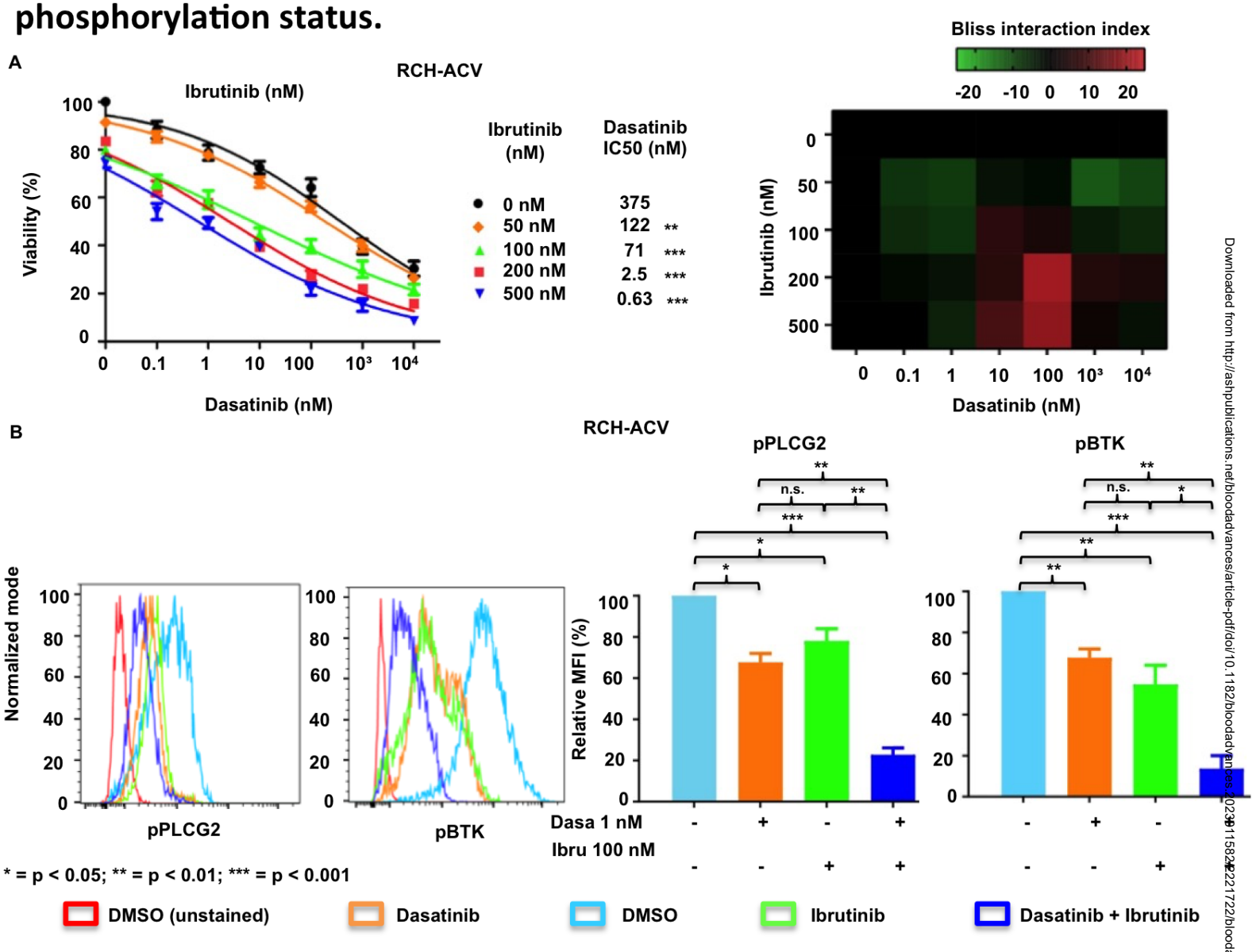

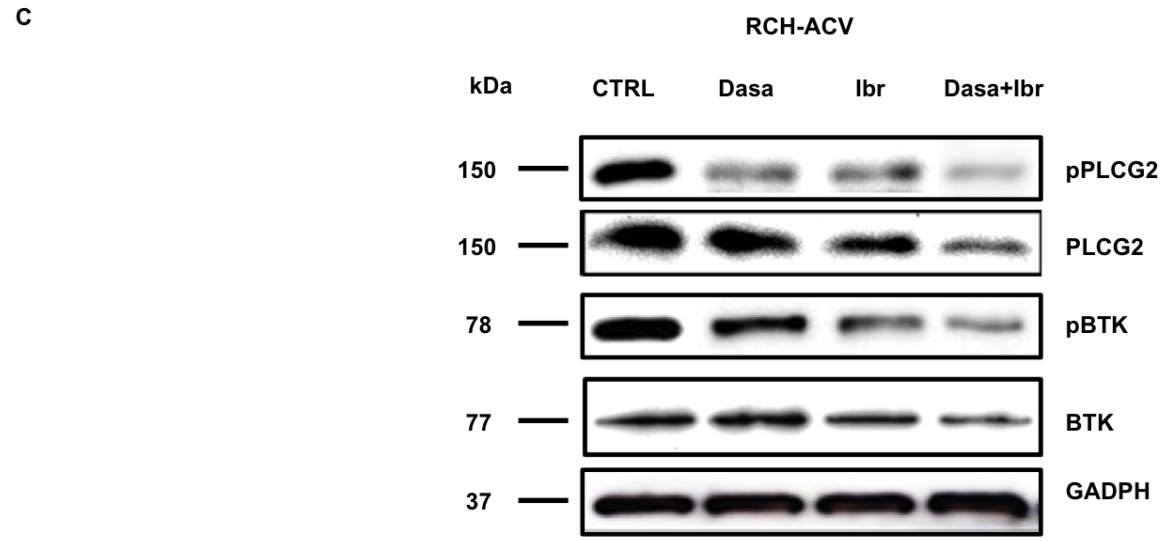

pPLCG2/PLCG2	0.89	0.57	0.64	0.63
PLCG2/GADPH	0.92	0.94	0.70	0.32
pBTK/BTK	1.70	1.19	0.96	0.90
BTK/GADPH	0.54	0.60	0.45	0.27

Figure 3

Figure 3. In vivo sensitivity of E2A-PBX1^{+}/preBCR^{+} leukemia cells to the combination dasatinib and BTKi.

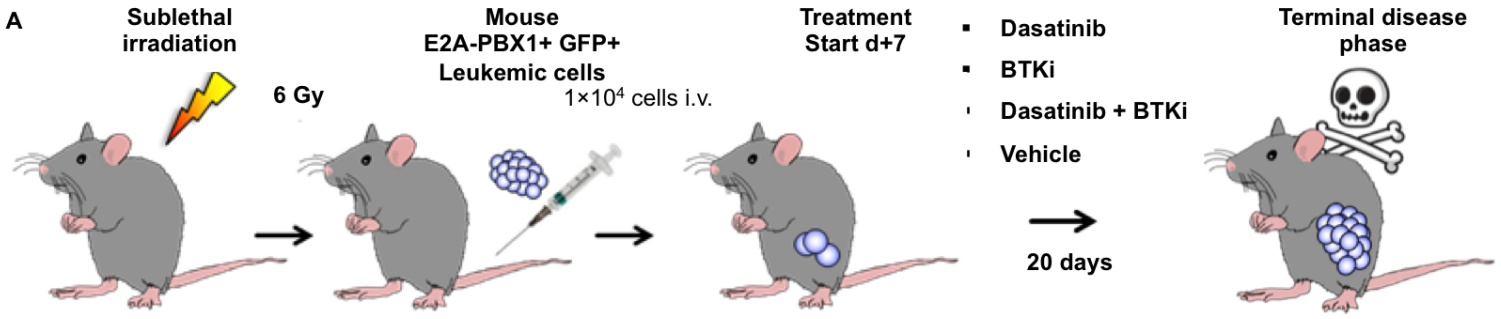

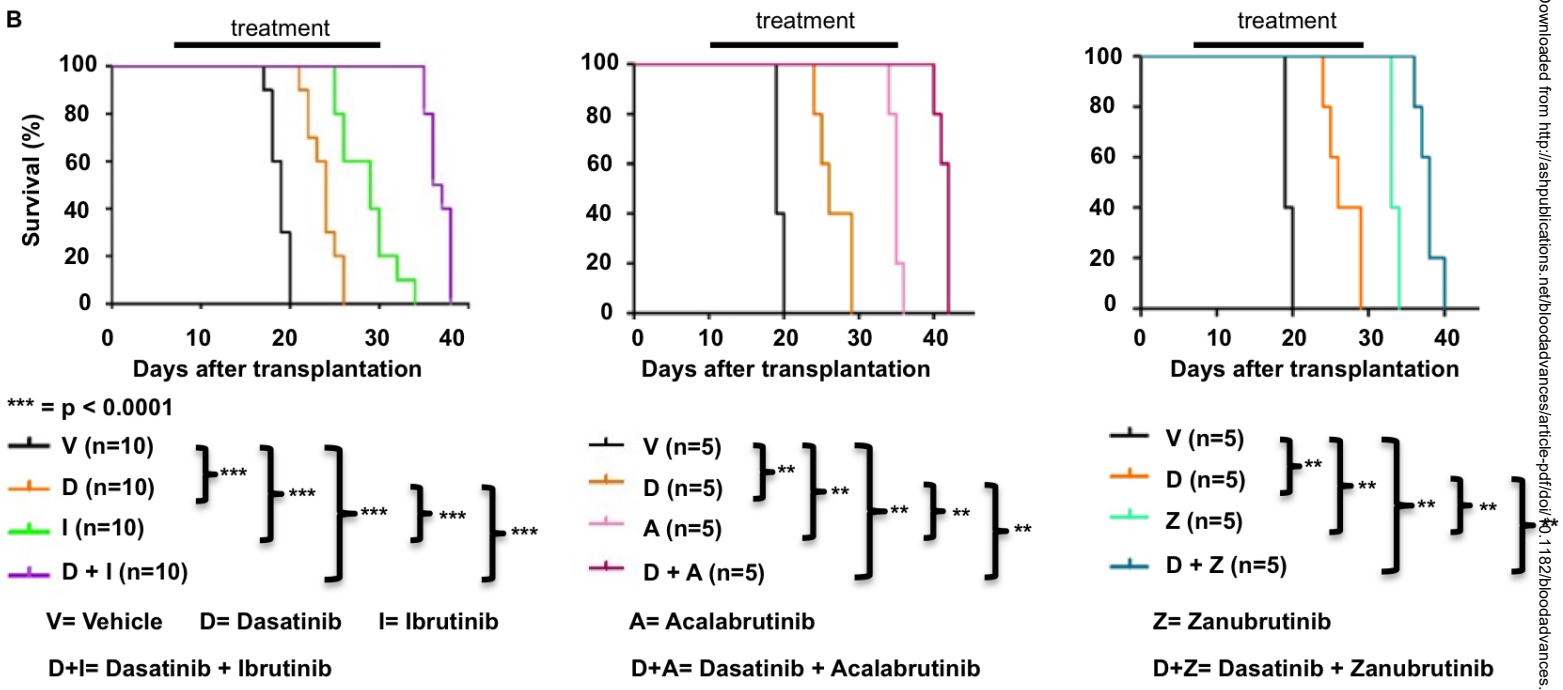

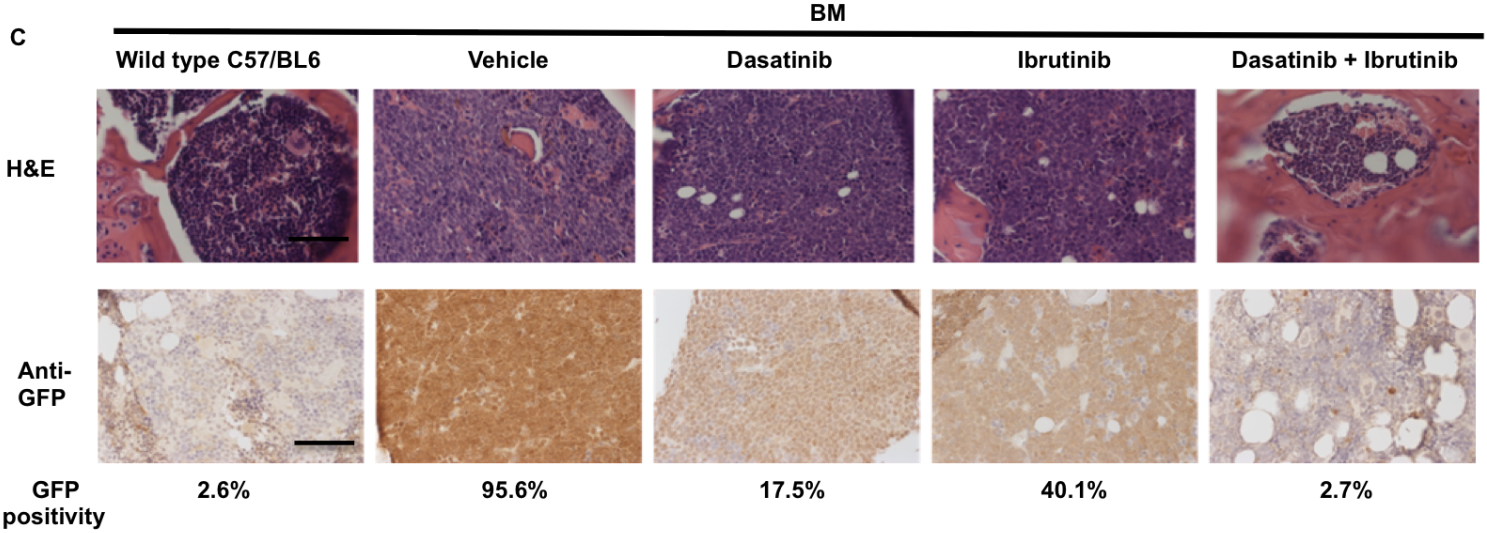

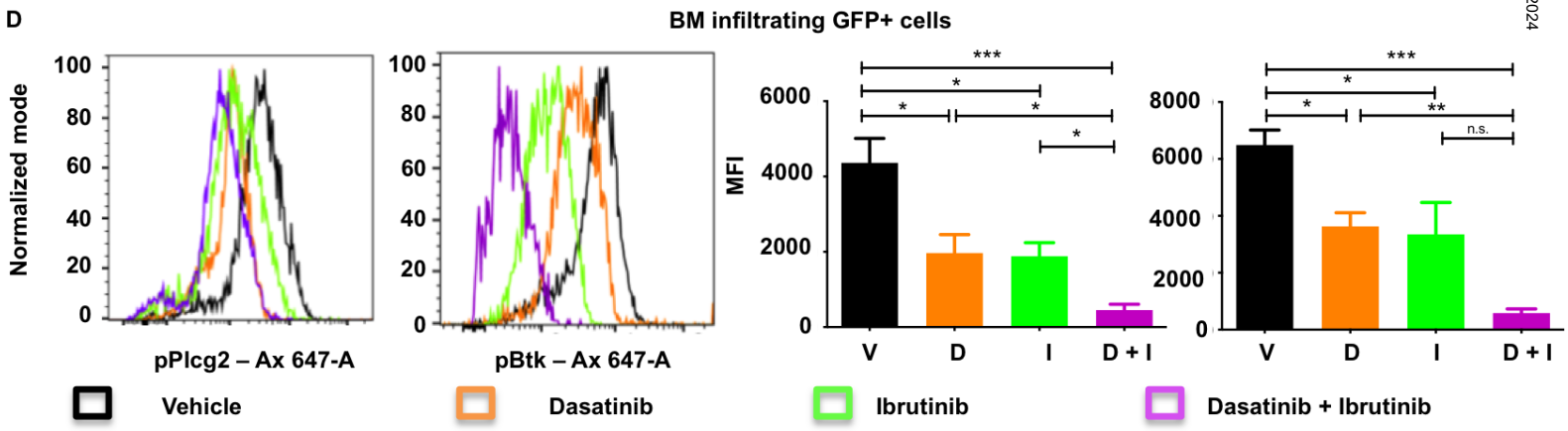

Figure 4

Figure 4. Decrease of leukemic CNS infiltration by combination therapy with dasatinib and BTKi.

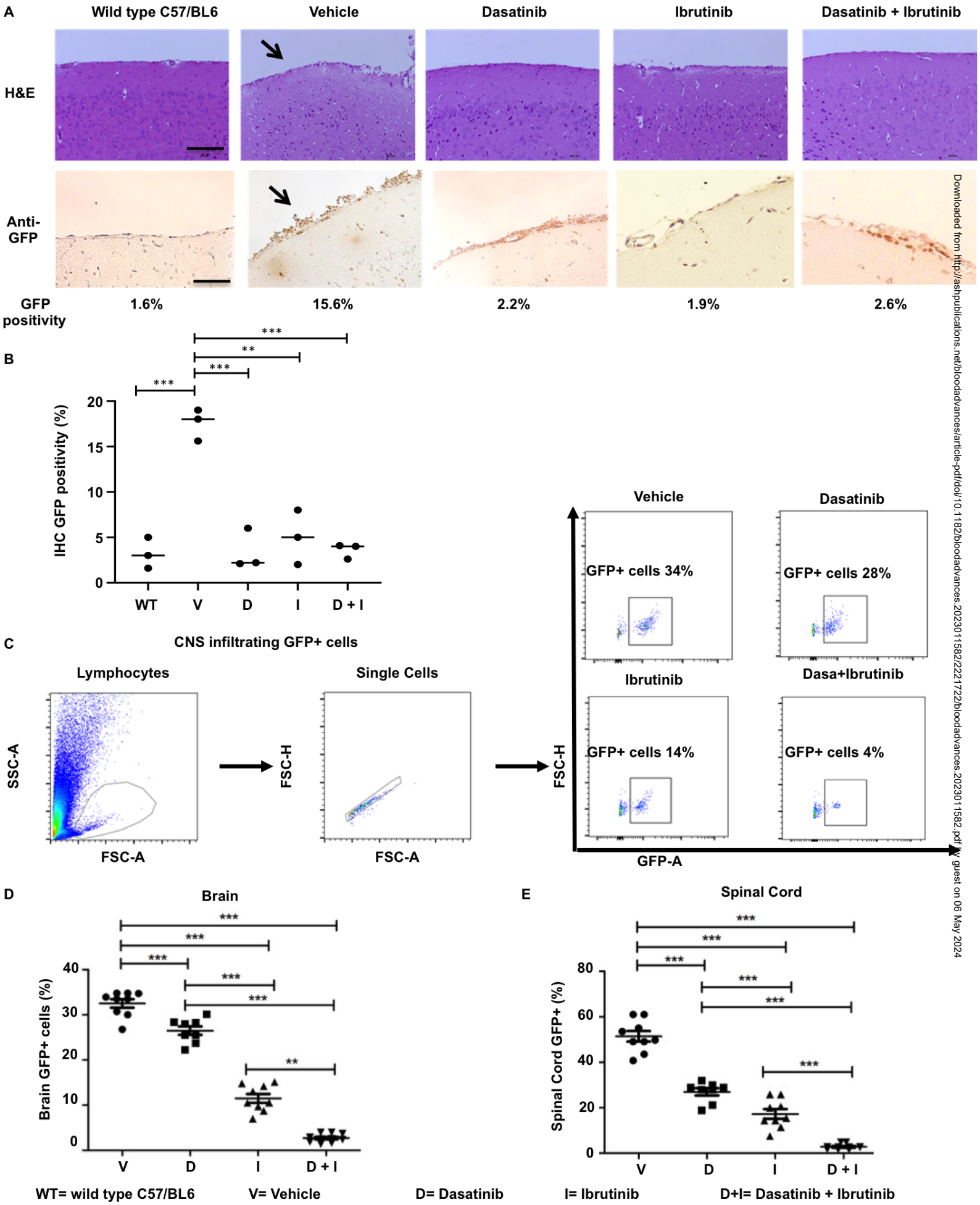

Figure 5

Figure 5. RNAseq of E2A-PBX1+/preBCR+ leukemia CNS-infiltrating cells compared across treatments.

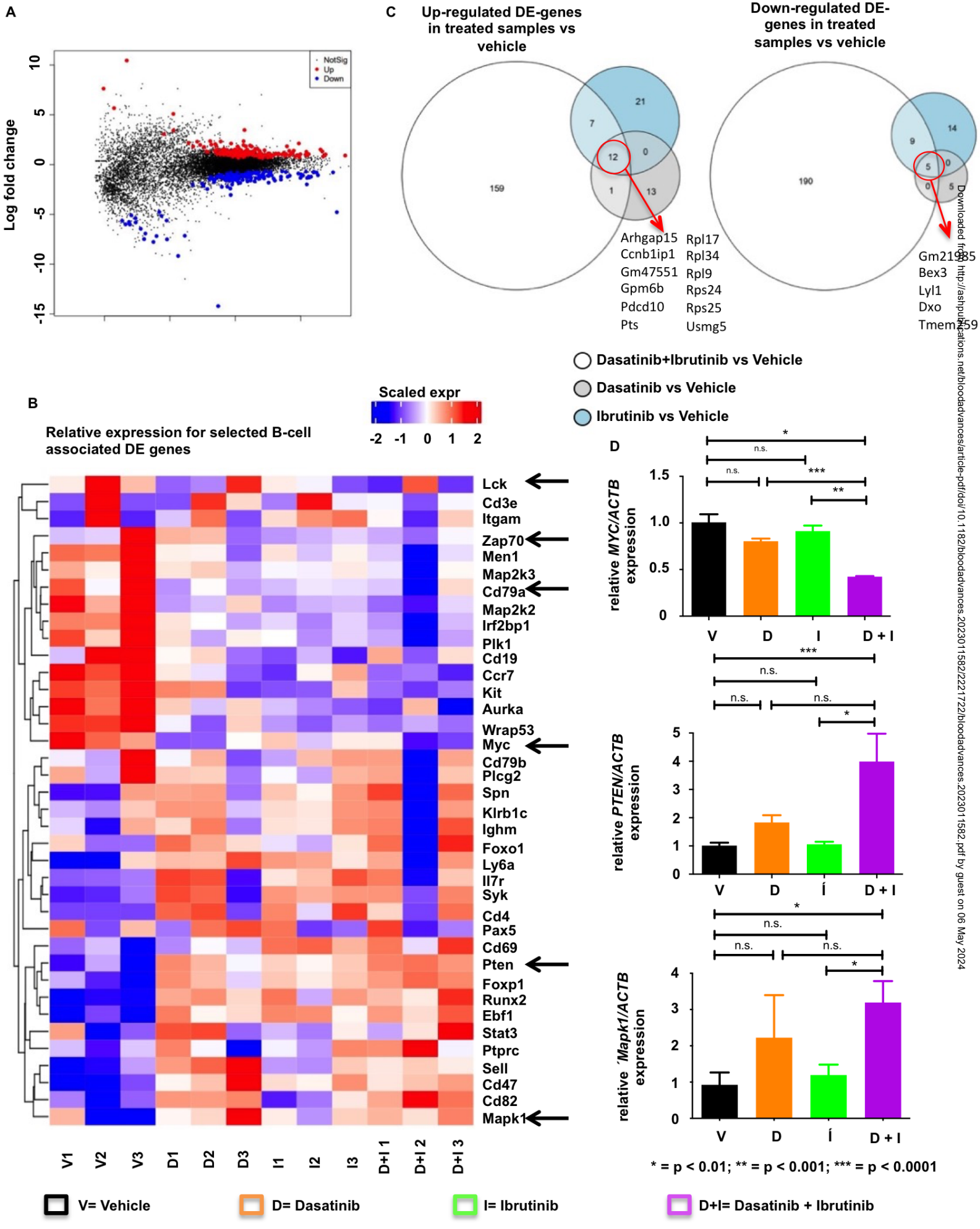

Figure 6

Figure 6 Effect of combined therapy with dasatinib and ibrutinib on human primary samples on PLCG2 and BTK phosphorylation status.